JOURNAL OF EXPERIMENTAL AND THEORETICAL PHYSICS, 2024, Vol. 165, No. 4, pp. 588–595

STATISTICAL, NONLINEAR, AND SOFT MATTER PHYSICS

GENERATION OF A FLAT STATIONARY SHOCK WAVE WITH EXTREMELY HIGH PRESSURE TRANSFER TO SOLID MATTER FROM A LOW-DENSITY ABSORBER OF TERAWATT LASER PULSE RADIATION

© 2024 I. A. Belov[a], S. A. Belkov[a], S. V. Bondarenko[a], G. A. Vergunova[b], A. Yu. Voronin[a], S. G. Garanin[a], S. Yu. Golovkin[a], S. Yu. Guskov[b], N. N. Demchenko[b], V. N. Derkach[a], N. V. Zmitrenko[c], A. V. Ilyushechkina[a], A. G. Kravchenko[a], A. A. Kuzina[a], I. V. Kuzmin[a], P. A. Kuchugov[c], A. E. Myusova[a], V. G. Rogachev[a], A. N. Rukavishnikov[a], E. Yu. Solomatina[a], K. V. Starodubtsev[a], P. V. Starodubtsev[a], I. A. Chugrov[a], O. O. Sharov[a], R. A. Yakhin[b,*]

[a]*Russian Federal Nuclear Center All-Russian Research Institute of Experimental Physics, 607188, Sarov, Nizhny Novgorod Region, Russia*

[b]*Lebedev Physical Institute of the Russian Academy of Sciences, 119991, Moscow, Russia*

[c]*Keldysh Institute of Applied Mathematics of the Russian Academy of Sciences, 125047, Moscow, Russia*

**e-mail: yakhin.rafael@gmail.com*

Received October 18, 2023
Revised November 17, 2023
Accepted November 20, 2023

Abstract. The generation of a powerful laser-induced shock wave in solid matter with a long period of stationary propagation of a flat front at extremely high pressure transfer from a low-density radiation absorber of a terawatt laser pulse to solid matter has been experimentally substantiated. The experiments were performed with flat targets containing an aluminum layer of various shapes and a laser radiation absorber layer made of porous material with a density of 0.01–0.025 g/cm^3. The targets were irradiated with second-harmonic Ndlaser pulses with an intensity of 10^{13}–$5 \cdot 10^{13}$ W/cm^2. Stationary propagation of flat shock waves in the aluminum layer was recorded at a velocity of 20–30 km/s for more than 1 ns with a near-maximum pressure increase from 3–3.5 Mbar in the absorber layer to 7–10 Mbar in the aluminum layer. The result significantly advances the possibilities of precise control over the spatial-temporal dynamics of shock waves in studies of the equation of state of matter.

Keywords: *shock wave, porous substance, laser plasma*

DOI: 10.31857/S004445102404e126

1. INTRODUCTION

One of the effective methods for generating powerful laser-induced shock waves (SW) in solid matter involves using a target containing a low-density laser pulse radiation absorber in the form of a porous material layer. This approach is based on the universal method of increasing SW pressure during its transition from a less dense medium to a denser one [1]. In turn, the porous material itself, which unlike a gaseous medium does not require special technical efforts for its use as a target element, possesses a set of important advantages related to laser radiation absorption and ablation pressure formation. These include the high absorption fraction of first to third harmonics of Nd-laser established in many experiments [2–7]: 80% in 90% porous media of light elements with both lower and higher density than the critical density of the formed plasma. Furthermore, radiation absorption in matter with supercritical density is a prerequisite for the formation of pressure higher than when laser pulse affects solid matter, where radiation can only be absorbed in plasma of subcritical density [8, 9].

Experiments demonstrated high efficiency of using porous material as a low-density absorber, in which the absorption of terawatt laser pulse radiation and initial shock wave generation occur. In works [10–13], a 2.5–3-fold increase in pressure was recorded in the aluminum layer compared to the pressure in the porous absorber. Targets in the form of an aluminum layer covered with a layer of porous TMPTA material ($C_{15}H_{20}O_6$) in a wide range of densities of the latter (2–10 mg/cm^3), were irradiated by sub-nanosecond duration laser pulses (400–600 ps) of second harmonic Nd-laser radiation and third harmonic I-laser with intensity about 10^{14} W/cm^2. In experiments [14, 15] when irradiating targets with a significantly longer pulse duration (3–4 ns) with more extended layers of porous TAC material absorber ($C_{12}H_{16}O_8$) with densities in the range 5–25 mg/cm^3, an even higher, record-breaking pressure increase of 3–3.5 times was achieved, close to the limit (about 4 times [12, 16]). The experiments were performed at the "Luch" facility at the Institute of Laser Physics Research of the Russian Federal Nuclear Center VNIIEF (ILFI RFNC-VNIIEF) by irradiating targets with TAC material using second harmonic Nd-laser radiation beam with energy of 200–600 J [17]. A known method for determining shock wave velocity in the aluminum layer was used. The target was a flat absorber layer combined with an aluminum layer about 20 μm thick (this design is called basic), with an additional step of the same material with thickness of 10–20 μm deposited on the rear side of the aluminum layer. The experiment measured the difference in time moments of shock wave exit to the rear side of the basic layer and to the rear side of the step. The shock wave velocity was determined as the ratio of step thickness to this time difference.

Fig. 1 shows summary data on measuring SW velocity in a single-stage aluminum layer in targets containing a layer of porous TAC absorber with densities of 5–25 mg/cm^3 and thicknesses from 200 to 400 μm (some of these data are presented in works [14, 15]), and in targets containing a solid lavsan absorber with density of about 1.3 g/cm^3 and thickness of 4 μm.

This work is devoted to studying the spatial-temporal dynamics of laser-induced SWs in targets that provide extremely high pressure transfer to solid matter from a low-density radiation absorber of a terawatt laser pulse. Controlling the duration of stationary SW propagation and its front shape is of

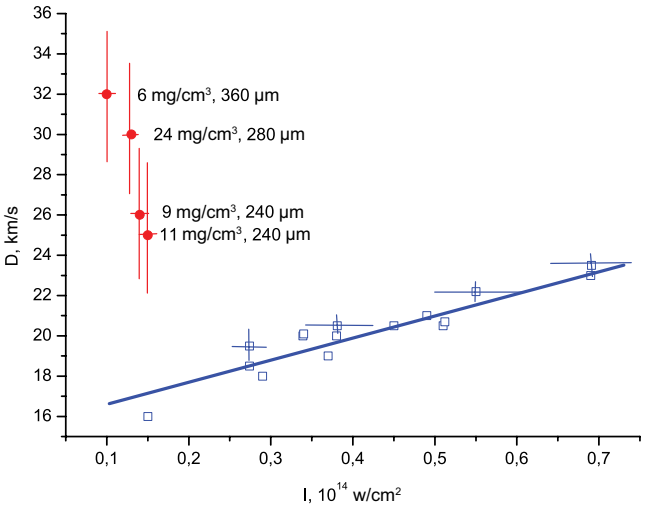

Fig. 1. (In color online.) Average SW velocities in aluminum, measured in experiments with targets containing an absorber in the form of a porous TAC-substance layer with thicknesses from 240 to 360 μm (red dots) and in the form of a 4 μm thick lavsan layer (blue squares)

fundamental importance for practical applications related to the study of the equation of state (EOS) of matter and laser thermonuclear fusion. Thus, the requirements of shock-wave experiments for EOS research are that the SW must remain flat and quasi-stationary throughout the entire measurement period. Furthermore, the wave must propagate through the target over a distance exceeding at least the spatial resolution of the diagnostic methods used, for a time exceeding at least their temporal resolution.

2. EXPERIMENTAL CONDITIONS

The experiments were performed at the "Luch" facility of ILFI RFNC-VNIIEF under irradiation conditions used in works [14, 15]. As in these works, targets containing a layer of porous TAC laser radiation absorber and a solid aluminum target part were used (Fig. 2). These target parts were separated by a vacuum gap, which resulted from the chosen target assembly technology. The porous TAC absorber was a fine-porous medium with a mixed membrane-filamentous structure of solid elements within open pores of about 0.5 μm. The average density and thickness of the absorber varied within 0.01–0.025 g/cm^3 and 200–400 μm, respectively. The absorber layer thicknesses significantly exceeded the geometric transparency length of TAC substance with the specified density. Two types of targets were used, which differed in the solid part structure: a flat layer was used to study spatial uniformity (time

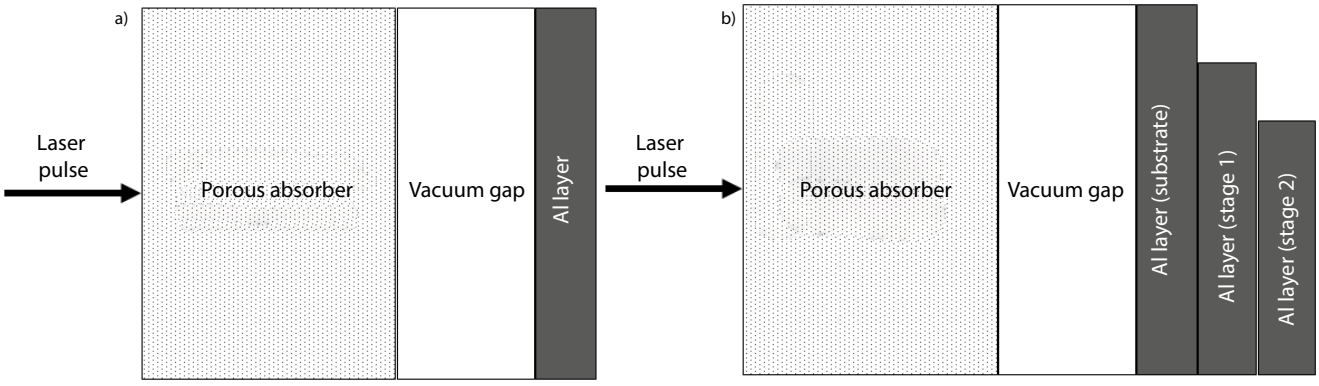

Fig. 2. Target scheme for measuring the time variance of SW exit on the rear surface of the aluminum layer (a) and target scheme for studying the temporal dynamics of SW (b)

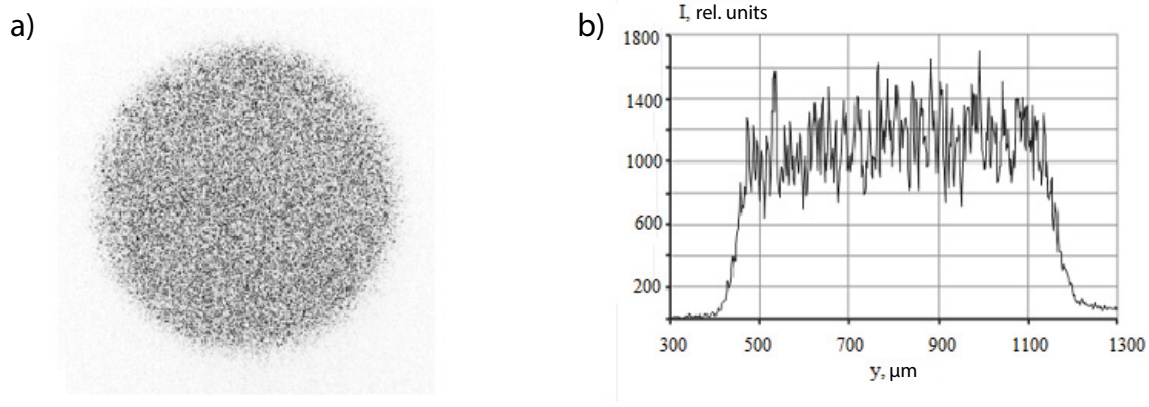

Fig. 3. Focusing spot (a) and its spatial distribution (b) on the target surface

variance) of SW in cross-section (Fig. 2a), and a flat layer supplemented with two steps, for measuring the average SW velocity at different depths of aluminum material (Fig. 2b). The moments of SW exit from the base layer and aluminum steps were recorded.

The thickness of the flat aluminum layer in all targets was approximately 20 μm, the maximum thickness including step thicknesses was about 50 μm. In the current series of experiments, the SW exit from the target was determined by plasma luminescence during vacuum unloading. Registration was carried out using a streak camera [18] based on a time-analyzing electron-optical converter with an 8 mm working field photocathode, brightness amplifier with microchannel plate and digital CCD camera with 1000×1000 elements matrix. The registration technique is described in detail in work [14], with temporal resolution of about 30 ps and spatial resolution of about 20 μm.

The method for determining the spatiotemporal structure of the SW front at the base layer output was as follows. Signal correction with background subtraction and convolution of the luminescence signal with the hardware function were performed. The coordinate array formed a signal isoline, defined as the SW front.

The targets were irradiated normally by second-harmonic pulses of Nd-laser with energy in the range of 200–400 J, with duration of about 4 ns, which, as before [14, 15], ensured SW generation under conditions of practically maximum pressure increase during SW transition from low-density absorber to solid matter. The temporal pulse shape was a trapezoid with intensity half-width duration from 3.4 to 3.8 ns and rising and falling parts durations of about 1.5–2.2 ns and about 1 ns respectively. To ensure uniform radiation intensity distribution in the beam focusing spot on the target surface, a phase plate was used, which formed a spot with diameter of 700 μm with uniform part diameter of about 600 μm (Fig. 3). The radiation intensity on the target surface in different experiments ranged from 10^{13} to $2 \cdot 10^{13}$ V/W cm^2. The maximum irradiation non-uniformity in the central part of the spot, considering

spatial scales larger than 50 μm, was no more than 14%, with root mean square of about 3–4%.

Numerical modeling was performed using a one-dimensional Lagrangian hydrodynamics program SND [19, 20] and a two-dimensional Eulerian hydrodynamics program NUTCY [21] for calculating the interaction of terawatt laser pulse with plasma. For these studies, the programs were supplemented with blocks for calculating the interaction of laser radiation with partially homogenized plasma of porous material. The absorption of radiation was calculated as a result of inverse bremsstrahlung process in the plasma volume at the depth of geometric transparency [22], depending on the duration of plasma homogenization in ion-ion collisions at a given point in plasma at a given time [23, 24]. In the equation of motion and energy equation, operators limiting the pressure gradient and electron thermal conductivity flux were used, which are also functions of homogenization duration [8, 24]. For the fine-porous absorber used in the discussed experiments, the calculation results differed insignificantly from the case of equivalent (in density and chemical composition) solid material. The shock wave propagation velocity in the porous absorber, with characteristic pore homogenization time of about 20 ps, decreased compared to solid material by no more than 10%.

3. SPATIOTEMPORAL CHARACTERISTICS OF SHOCK WAVE PROPAGATION IN LOW-DENSITY POROUS MATERIAL

Table 1 presents the experimental conditions and results, as well as numerical calculation results related to the study of SW spatial structure in the transverse direction. The measured time differences $\Delta\tau$ of SW emergence on the surface of 20 μm thick aluminum layer at the center and edge of the laser beam focusing spot range from 20 to 50 ps.

Fig. 4 shows, as an example, the registration of the SW front and its processing results in experiment No. 3 from Table 1. Fig. 4b shows the spatial distributions of luminescence signals for different SW fragments. The figure also shows the shape of the target irradiation pulse (section 3), its temporal alignment with the SW chronogram was carried out using data from the calibration experiment (without target).

The measured timing difference values $\Delta\tau$ were used to calculate the relative decrease in SW velocity in the spot cross-section. For this purpose, two-dimensional numerical calculations performed using the NUTCY program were used. Table 1 shows the ratio of SW velocity difference between the center and edge of the spot on the rear surface of the aluminum layer to the average SW velocity V_c in aluminum along the laser beam axis, obtained in calculations using the NUTCY program: $\delta V_{ex}/V_c = V_c\Delta\tau/h_0$. The relative decrease in SW velocity at the spot edge determined in this way does not exceed 6%, which indicates a flat SW front within the focusing spot of the "Luch" laser facility. The values $\delta V_s/V_c$ from numerical calculations shown in Table 1 are close to the values $\delta V_{ex}/V_c$ determined from the measured timing differences $\Delta\tau$.

The highest SW velocity in the aluminum layer $V_c = 28$ km/s occurs in the calculation of experiment

Table 1. Experimental conditions and results, as well as numerical calculation results for the study of spatial distribution of SW velocity: h_p and ρ – thickness and average density of porous absorber; h_g – thickness of vacuum gap between porous absorber layer and aluminum layer; h_0 – thickness of aluminum layer; $E_{2\omega}$ – second harmonic laser pulse energy in the irradiation spot; I – laser radiation intensity in the central uniform part of the spot; $\Delta\tau$ – time difference of SW emergence at the center and edge of the spot; $\delta V_{ex}/V_c$ – difference in SW velocities at the center and edge of the spot, calculated from time difference $\Delta\tau$ and normalized to SW velocity at the center of the spot in 2D numerical calculation; V_c – SW velocity at the center of the focusing spot in 2D numerical calculation; $\delta V_s/V_c$ – difference in SW velocities at the center and edge of the spot, normalized to SW velocity at the center of the focusing spot in 2D numerical calculation V_c

No.	h_p, μm	ρ, mg/cm^3	h_g, μm	h_0, μm	$E_{2\omega}$, J	I, 10^{13} W/cm^2	$\Delta\tau$, ps	$\delta V_{ex}/V_c$	V_c, km/s	$\delta V_s/V_c$
1	304	10	47	20	260	1.5	40	0.055	28	0.0
2	361	9	43	20	210	1.2	20	0.024	24	0.0
3	222	9	64	20	200	1.2	50	0.052	21	0.0

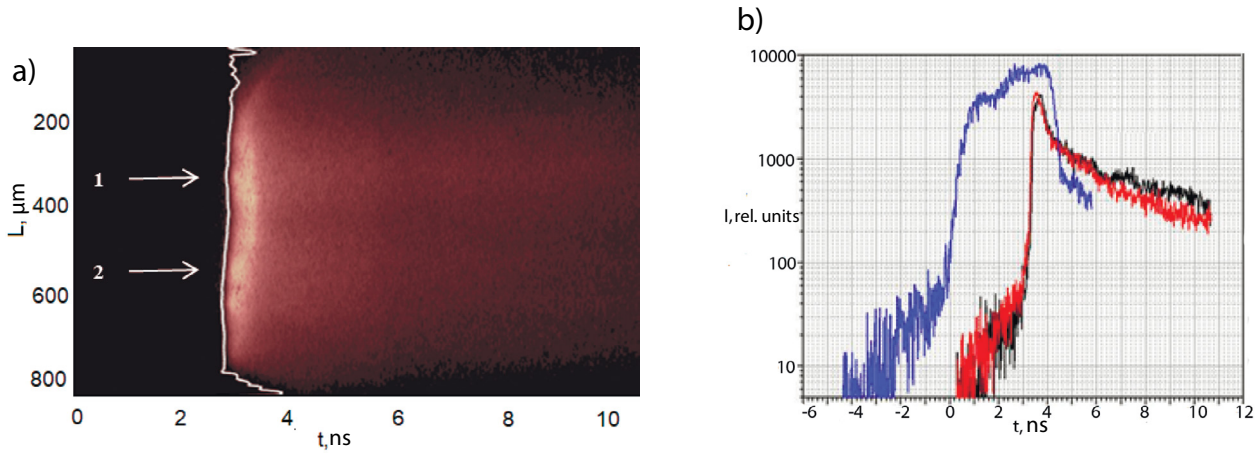

Fig. 4. (In color online) a) Chronogram of SW luminescence in experiment No. 3 from Table 1: white curve – isoline of SW front output. b) Time dependencies of luminescence for different transverse coordinates of a flat-type target: black curve – section 1, red curve – section 2, blue curve – section 3 (laser pulse mark)

No. 1 at the maximum laser pulse intensity $1{,}5\cdot10^{13}$ W/cm^2. The velocity V_c slightly decreases to 24 km/s in the calculation of experiment No. 2 when the intensity decreases to $1.2\cdot10^{13}$ W/cm^2. The target in experiment No. 2 had, like the target in experiment No. 1, a sufficiently thick absorber layer and a similar ratio of absorber thickness to vacuum gap thickness, $h_p/h_g = 8.4$. In the calculation of experiment No. 3, the velocity V_c decreased to 21 km/s under otherwise equal conditions compared to calculation No. 2, except for the ratio h_p/h_g, which in experiment No. 3 was significantly lower – 3.4. The presence of a thinner porous absorber layer (with an increased gap) causes a decrease in SW velocity in aluminum in experiment No. 3 due to the early arrival of the unloading wave from the low-density material layer. The results of experiment No. 2 show that it achieved the best degree of velocity distribution uniformity $\delta V_{ex}/V_c = 0.024$, while numerical calculation does not significantly distinguish experiment No. 2 compared to experiments No. 1 and No. 3 in terms of $\delta V_s/V_c$. Experiment No. 2 differed from experiments No. 1 and No. 3 in that it had the highest ratio h_p/h_g.

In Fig. 5, as an example of numerical calculations using the NUTCY program, the density and pressure distributions are shown for experiment No. 1 conditions at 3 ns, when the SW front in the beam center reaches the rear surface of the aluminum layer. The laser beam falls normally (in Fig. 5 from top to bottom) on the surface of the absorber layer with density 10 mg/cm^3, which initially occupied the region with coordinate z from 167 to 471 μm, followed by vacuum gap with density 10^{-6} g/cm^3 (at z from 120 to 167 μm), and then aluminum layer – (at z from 100 to 120 μm). By 3 ns in the beam center, the average SW velocity is 28 km/s, pressure behind its front is about 7.5 Mbar, which is approximately 3 times higher than the pressure behind the SW front during its propagation in the porous material layer. The difference in wave front position between center and edge of laser beam is about 2 μm, corresponding to a delay of about 70 ps.

To estimate the ablation pressure value in low-density absorber, the known scaling [25, 26] can be used for the case of laser pulse impact on matter with supercritical density $\rho > \rho_{cr}$. This is due to the fact that absorber densities of 10 mg/cm^3 and 9 mg/cm^3 are less than critical density by only 1.2 and 1.4 times respectively, and after SW generation, laser radiation will affect matter with supercritical density. The scaling for ablation pressure has the form

$$P_{ab}[\text{Mbar}] \approx \rho_{cr}\left[\frac{2(\gamma-1)}{3\gamma-1}\frac{I}{\rho_{cr}}\right]^{2/3} \approx \approx 12\left[\frac{2(\gamma-1)}{3\gamma-1}\right]^{2/3}\left(\frac{A}{Z}\right)^{1/3}\frac{I_{(14)}^{2/3}}{\lambda_\mu^{2/3}}, \quad (1)$$

where $\rho_{cr} \approx 1.8\cdot10^{-3}A/Z\lambda_\mu^2$ critical density in g/cm^3, A and Z – atomic number and plasma ionization degree, λ_μ is wavelength in μm, $I_{(14)}$ is intensity in units 10^{14} W/cm^2, γ is adiabatic index.

In the approximation of fully ionized absorber plasma ($A/Z \approx 2$, $\gamma = 5/3$) at $\lambda_\mu = 0.53$ μm for

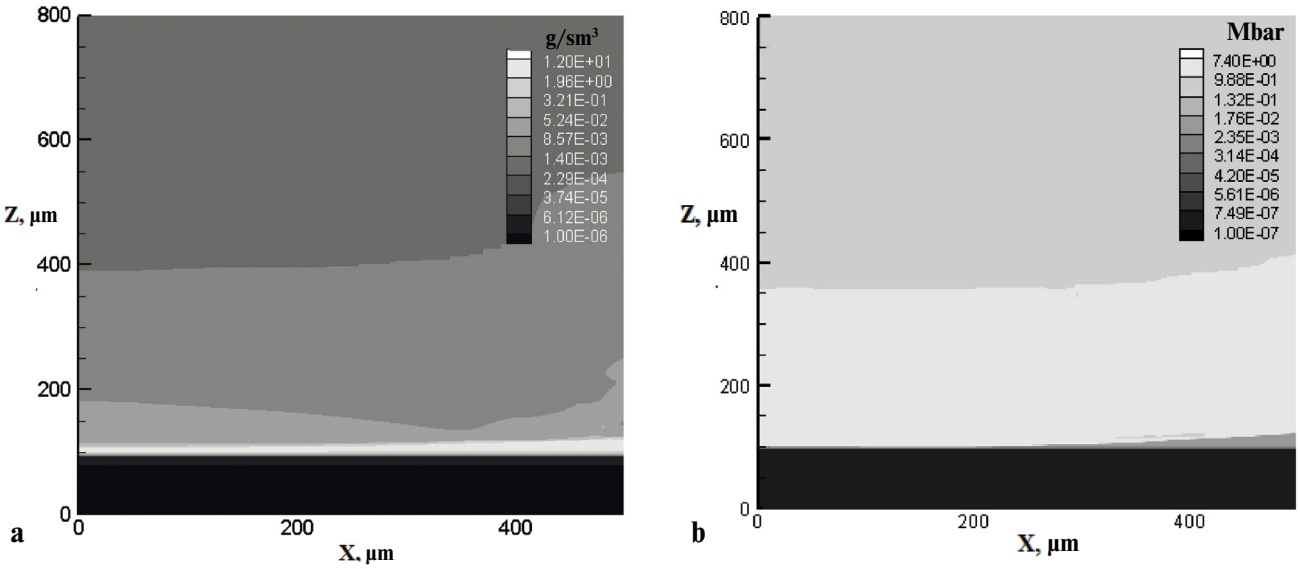

Fig. 5. Distributions of density (a) and pressure (b) at 3 ns (calculation using NUTCY program)

$I = 0.15 \cdot 10^{14}$ W/cm^2 estimation using formula (1) gives a value of $P_{ab} = 3.2$ Mbar, which is in good agreement with numerical calculation results. The approximate estimation of pressure increase during shock wave transition from absorber with density ρ_a to solid material layer with density ρ_s is given by expression [12, 16]

$$G \approx \left[\frac{\left(1+\beta^{1/2}\right)}{\left(1+\beta^{1/2}\dfrac{\rho_a}{\rho_s}\right)} \right]^2, \qquad (2)$$

where $\beta = \left(1+\gamma_a\right)/\left(1+\gamma_s\right)$, γ_a and γ_s are adiabatic indices in the absorber and solid part of the target. When the absorber density is much lower than the solid part density, $\rho_a \ll \rho_s$, expression (2) gives a scale of maximum pressure increase of about 4. The shock wave pressure in aluminum of 7.5 Mbar, obtained in numerical calculations considering real aluminum EOS, corresponds to pressure increase compared to absorber pressure (3.5 Mbar) by approximately 3 times, which is close to the maximum.

Table 2 presents the experimental conditions and results, as well as numerical calculations related to the study of SW temporal dynamics performed using targets containing a two-step aluminum layer.

Fig. 6 shows, as an example, a chronogram of experiment No. 6 from Table 2, which demonstrates SW propagation through the steps.

The experimental results indicate a high degree of SW propagation stationarity over a distance of about 30 μm during a time period of up to 1.5 ns. The decrease in SW velocity in the second aluminum step was no more than 10–15% of the SW velocity in the first step. Such a high degree of SW stationarity and such insignificant distortion of its front spatial shape more than satisfactorily meet the spatial and temporal resolution capabilities of diagnostic methods used in modern EOS experiments. Numerical calculations were performed using the SND one-dimensional program, the use of which is justified by results indicating a flat SW front. The calculation results show good agreement with experimental results.

4. CONCLUSION

The high efficiency of using a low-density radiation absorber of terawatt laser pulse with nanosecond duration for generating a flat stationary SW with extremely high pressure transfer from the absorber to solid matter has been experimentally validated. For conditions relevant to EOS research, the duration of stationary SW propagation in solid matter and the degree of preservation of such wave's flat front have been established.

When irradiating targets containing a porous absorber layer with density 0.01–0.025 g/cm^3 and thickness from 200 to 400 μm, using second harmonic Nd-laser radiation pulse withintensity

Table 2. Experimental conditions and results, as well as numerical calculation results for studying the temporal dynamics of shock wave velocity: h_p and ρ – thickness and average density of the porous absorber; h_g – vacuum gap thickness between the porous absorber layer and aluminum layer; h_0, h_1 and h_2 – thickness of the base layer and aluminum layer steps; $E_{2\omega}$ – second harmonic laser pulse energy in the irradiation spot; I – laser radiation intensity in the central uniform part of the spot; Δt_1 and Δt_2 – time difference between shock wave exit from the base layer and first step, and between first and second steps; $V_{1(ex)}$ and $V_{2(ex)}$ – average shock wave velocities in the first and second steps, measured experimentally; $V_{1(c)}$ and $V_{2(c)}$ – average shock wave velocities in the first and second steps calculated using the SND program

No.	h_p, μm	ρ, mg/cm^3	h_g, μm	h_0; h_1; h_2, μm	$E_{2\omega}$, J	I, 10^{13} W/cm^2	Δt_1; Δt_2, ps	$V_{1(ex)}$; $V_{2(ex)}$, km/s	$V_{1(c)}$; $V_{2(c)}$ km/s
1	348	10	53	20; 13; 12	210	1.3	580; 540	23.3; 22.6	
2	339	10	41	20; 14; 16	180	1.1	630; 740	23.2; 21.5	
3	323	20	23	20; 12; 10	190	1.1	510; 550	22.9; 21.3	
4	280	24	22	20; 16; 16	310	1.3	720; 710	21.9; 22.8	
5	283	24	22	20; 11; 11	320	1.6	390; 470	29.7; 25.1	
6	300	25	38	20; 16; 13	420	1.8	580; 590	27.4; 22.2	

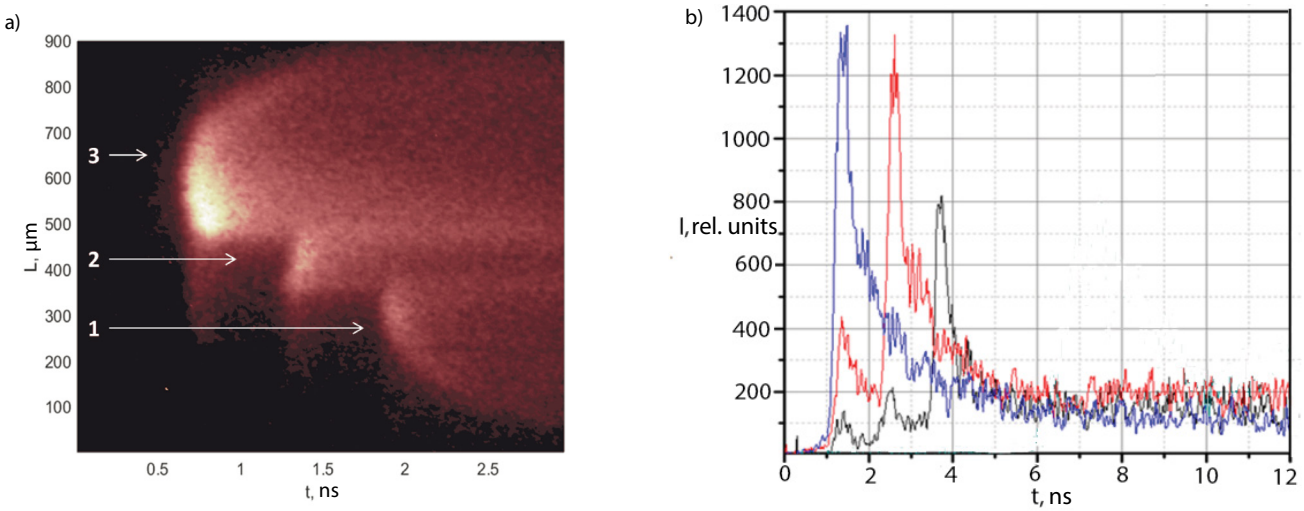

Fig. 6. (In color online) Chronogram of SW luminescence in experiment No. 6 from Table 2 (a) and temporal dependencies of luminescence for different transverse coordinates of flat-type target (b). Black curve – section 1, red curve – section 2, blue curve – section 3

about 10^{13} W/cm^2, stationary propagation of flat SWs in the aluminum layer was recorded at a velocity of 20–23 km/s, with transverse variation not exceeding 5%, during a time period exceeding 1 ns, with near-maximum pressure increase from 3–3.5 Mbar in the absorber layer to 7–10 Mbar in the aluminum layer. Such high degree of SW stationarity and insignificant distortion of its front spatial shape more than satisfy the requirements of modern EOS experiments.

Given the known dependence of pressure initiating SW on the intensity and wavelength of the incident laser radiation $P \propto \left(I/\lambda\right)^{2/3}$ [25, 26], with a tenfold increase in pulse intensity, one can predict an increase in the pressure of a stationary plane SW by 4.5 times – up to 40 Mbar for the second harmonic of Nd-laser radiation and by 6 times – up to 50 Mbar for the third harmonic.

FUNDING

The study was carried out within the framework of the scientific program of the National Center for Physics and Mathematics (project "Physics of High Energy Densities. Stage 2023-2025").

REFERENCES

1. Ya. B. Zeldovich, Yu. P. Raizer Physics of Shock Waves and High-Temperature Hydrodynamic Phenomena, Fizmatlit, Moscow (2008).
2. A. E. Bugrov, I. N. Burdonskii, V. V. Gavrilov et al., Laser and Part. Beams 17, 415 (1999).
3. A. Caruso, C. Strangio, S. Yu. Gus'kov, V. B. Rozanov, Laser and Part. Beams 18, 25 (2000).
4. T. Hall, D. Batani, W. Nazarov et al., Laser and Part. Beams 20, 303 (2002).
5. Ph. Nicolaï, M. Olazabal-Loumé, S. Fujioka et al., Phys. Plasmas 19, 113105 (2012).
6. S. Depierreux, C. Labaune, D. T. Michel et al., Phys. Rev. Lett. 102, 195005 (2009).
7. M. Tanabe, H. Nishimura, S. Fujioka et al., Appl. Phys. Lett. 93, 051505 (2008).
8. S. Yu. Gus'kov, M. Cipriani, R. De Angelis et al., Plasma Phys. Controll. Fusion 57, 125004 (2015).
9. R. De Angelis, F. Consoli, S. Yu. Gus'kov et al., Phys. Plasmas 22, 072701 (2015).
10. A. Benuzzi, M. Koenig, J. Krishnan et al., Phys. Plasmas 5, 2827 (1998).
11. M. Temporal, S. Atzeni, D. Batani, and M. Koenig, Euro. Phys. J. D 12, 509 (2000).
12. D. Batani, A. Balducci, W. Nazarov et al., Phys. Rev. E 63, 046410 (2001).
13. J. Limpouch, N. N. Demchenko, S. Yu. Gus'kov et al., Plasma Phys. Controll. Fusion 46, 1831 (2004).
14. I. A. Belov, S. A. Belkov, S. V. Bondarenko et al., JETP 161, 403 (2022).
15. S. A. Belkov, S. G. Garanin, V. G. Rogachev, S. Yu. Gus'kov, High-Power Lasers, Research in High Energy Density Physics, Proceedings of the XLVIII International (Zvenigorod) Conference on Plasma Physics and Controlled Thermonuclear Fusion (2021).
16. S. Yu. Gus'kov, H. Azechi, N. N. Demchenko et al., Plasma Phys. Controll. Fusion 51, 095001 (2009).
17. S. G. Garanin, A. I. Zaretsky, R. I. Ilkaev et al., QE 35, 299 (2005).
18. D. S. Kornienko, A. G. Kravchenko, D. N. Litvin et al., PTE 2, 78 (2014).
19. S. A. Belkov, G. V. Dolgoleva, Problems of Atomic Science and Technology, ser. Mathematical Modeling of Physical Processes 1, 59 (1992).
20. S. A. Belkov, S. V. Bondarenko, E. I. Mitrofanov, KE 30, 963 (2000).
21. V. F. Tishkin, V. V. Nikishin, I. V. Popov, A. P. Favorskiy, Mathematical Modeling 7, 15 (1995).
22. S. Yu. Guskov, V. B. Rozanov, KE 24, 715 (1997).
23. S. Yu. Gus'kov, J. Russian Laser Res. 31, 574 (2010).
24. M. Cipriani, S. Yu. Gus'kov, R. De Angelis et al., Laser and Part. Beams 36, 121 (2018).
25. Yu. V. Afanasiev and S. Yu. Gus'kov, in: Nuclear Fusion by Inertial Confinement. A Comprehensive Treatise, ed. by G. Velarde et al., CRC Press (1992), p. 99.
26. J. Lindl, Phys. Plasmas 2, 3933 (1995).